Journal of ELECTRICAL ENGINEERING, VOL. 53, NO. 1-2, 2002, 10–16

INFLUENCE OF THE MEYER–NELDEL RULE ON CHARGE DEEP LEVEL TRANSIENT SPECTRA

Peter Kluvánek * — **Drahoslav Barančok** * — **Vojtech Nádaždy** **

The impact of the Meyer-Neldel rule (MNR) on charge deep-level transient spectroscopy (QDLTS) of continuously distributed energy levels is investigated. We performed computer simulations of QDLTS spectra for a box-shaped energy distribution G(E) considering MNR via energy dependence of the exponential prefactor τ_0 of the charge emission rate defined by $\tau_0 = \tau_{00}\exp(-E/E_0)$. The main feature of these simulations is that below the critical temperature $T_0 = E_0/k$ the QDLTS spectra do not become broader with increasing the rate window as those observed for the distribution $G(E)$ with energy independent τ_0. To justify the viability of this description, we measured the continuum of interface states of two MOS structures prepared on crystalline silicon (c-Si) and undoped hydrogenated amorphous silicon (a-Si:H) substrates. Performed simulations were related to QDLTS spectra measured with large-pulse excitation which give a response from a wide energy interval. Unlike the former sample, QDLTS spectra of a-Si:H sample did not broaden with increasing the rate window. Their behaviour can be interpreted by MNR underlain in the prefactor τ_0 providing support for our consideration. Using a small-signal QDLTS method, which measures a limited fraction of the interface state continuum, the dependence of τ_0 on the activation energy E was constructed for both samples. It yielded the energy independent τ_0 and MN energy $E_0 = 0.38$ eV for interface states measured on c-Si and a-Si:H samples, respectively.

K e y w o r d s: Meyer-Neldel rule, undoped hydrogenated amorphous silicon, charge deep-level transient spectroscopy, crystalline silicon.

1 INTRODUCTION

Deep-Level Transient Spectroscopy (DLTS) [1] and its various modifications [2–5] have been successfully used for studying a wide class of thermally stimulated relaxation processes, *eg*, related to deep energy levels in crystalline [6–8] and amorphous [9–11] semiconductors, dielectric relaxations in insulators [12], *etc*. The principle of DLTS resides in repeated filling and emptying of the deep levels in the space-charge region of the Schottky barrier or metal-oxide-semiconductor (MOS) structure by means of voltage pulses and in monitoring the related response. The charge released from the deep levels can be detected either as a change of the depletion layer capacitance or of the current which flows in an external circuit. The released charge can also be detected by integrating the current in the external circuit over time [4, 5]. Under the assumption of an exponential response the DLTS signal [1] from a discrete level is defined as the difference of the measured quantity S (capacitance, current or charge) sampled at points in time t_1 and t_2 after the trailing edge of the excitation pulse plotted *versus* temperature T, *ie*,

$$\Delta S = S(t_1) - S(t_2) = \Delta S_0\left[\exp\left(-\frac{t_1}{\tau}\right) - \exp\left(-\frac{t_2}{\tau}\right)\right]. \quad (1)$$

The constant ΔS_0 is the amplitude of the measured transient and the time constant τ is given by the relation

$$\tau = \tau_0 \exp\left(\frac{E}{kT}\right), \quad (2)$$

where k is the Boltzmann constant and E is an activation energy of the discrete level. A well known expression relates τ_0 to more fundamental parameters [13] of the deep level

$$\tau_0 = \left(\sigma_n \langle v_n \rangle N_C\right)^{-1} \quad (3)$$

where σ_n is the electron capture cross section of the defect, $\langle v_m \rangle$ is the average thermal velocity of electrons, and N_C is the effective density of conduction band states. A usual temperature dependence of $\langle v_n \rangle$ and N_C is considered, *ie*, $\langle v_n \rangle N_C \propto T^2$ [13]. Since the time constant τ is thermally activated, there is a DLTS peak at the temperature T_m where the condition $\tau_m = (t_2 - t_1)/\ln(t_2/t_1)$ is fulfilled [1]. The activation energy E and τ_0 are determined by means of an Arrhenius' plot $\ln \tau_m$ *versus* $1/T_m$. This Lang's approach is a standard procedure used for determination of deep level parameters from DLTS spectra. In the case of exponential response these parameters can also be calculated from the full width at the half maximum (FWHM) of the DLTS peak.

In this contribution, we demonstrate how the presence of the Meyer-Neldel rule (MNR), *ie*, the exponential relation between the exponential prefactor of the underlying thermally stimulated quantity and thermal activation energy, can influence charge DLTS (QDLTS) spectra originating from continuously distributed energy levels. We briefly review the impact of the MNR on QDLTS discussed theoretically in recent papers [15, 16]. Considering MNR via energy dependence of the exponential prefactor

* Department of Physics, Faculty of Electrical Engineering and Information Technology, Slovak University of Technology, Ilkovičova 3, 812 19 Bratislava, Slovakia, e-mail: kluvanek@elf.stuba.sk

** Institute of Physics, Slovak Academy of Science, Dúbravská cesta 9, 842 28 Bratislava, Slovakia

ISSN 1335-3632

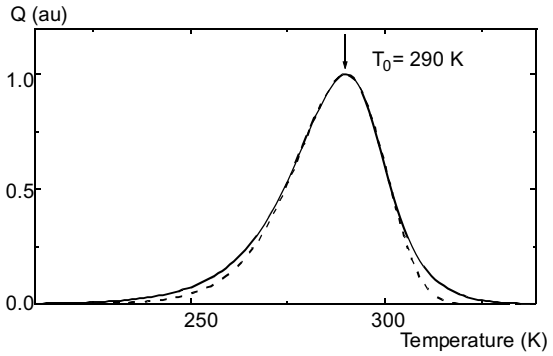

Fig. 1. Squeezing of the QDLTS spectrum (full line) due to the presence of the MNR calculated for a box-shaped energy distribution function $G(E)$ in the interval of $\langle 0.3, 0.9\rangle$ eV, $E_0 = 25$ meV, and $\tau'_{00} = 1\,\mathrm{sK}^2$. For comparison, QDLTS spectrum calculated for a discrete energy level $E = 0.6$ eV and $\tau'_0 = 3.78 \times 10^{-11}\,\mathrm{sK}^2$ (dashed line) is shown. Maxima of the QDLTS spectra occur for the sampling times $t_1 = 8.24 \times 10^{-6}$ s and $t_2 = 2t_1$ at the isokinetic temperature $T_0 = 290$ K.

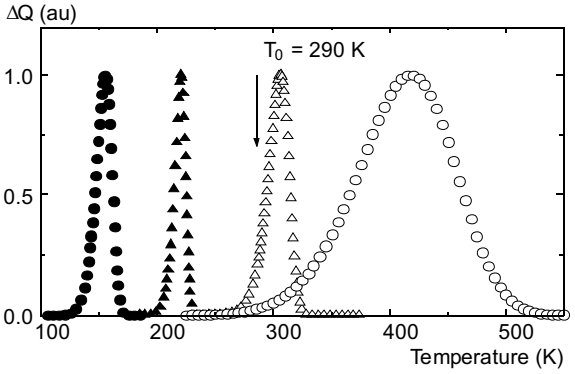

Fig. 2. Change of the sequence of QDLTS spectrum components above the isokinetic temperature due to the MNR impact is demonstrated by QDLTS peaks of discrete energy levels $E = 0.3$ eV (circle) and $E = 0.9$ eV (triangle). Full and open symbols correspond to sampling times t_1 of 10^{-1} s and 10^{-7} s, respectively. Other parameters: $E_0 = 25$ meV, $\tau'_{00} = 1\,\mathrm{sK}^2$.

τ_0 of the charge emission rate, computer simulations of QDLTS spectra for a box-shaped energy distribution are carried out. Experimental verification of this consideration is supported by QDLTS measurements of interface states at the oxide/undoped hydrogenated amorphous (a-Si:H) interface, which conform with the simulated spectra influenced by MNR. For comparison, the behavior of the interface states with energy independent τ_0 is illustrated on the MOS structure with crystalline silicon (c-Si).

2 THEORETICAL BACKGROUND

The compensation law, or MNR, has been known as an empirical result since 1937 [14]. This law is obeyed by many processes including annealing phenomena [17] and electronic processes in amorphous semiconductors [18, 19], charge trapping in crystalline semiconductors [20], conductivity in ionic crystals [21], aging of insulating polymers [22], and chemical reactions [23]. The MN rule describes a wide category of thermally activated processes for which a measured property X is given by [24, 25]

$$X = X_0 \exp\Big(-\frac{E}{kT}\Big) \quad \text{and} \quad X_0 = X_{00}\exp(bE)\,. \qquad (4)$$

Here X_{00} and b are positive constants, E is the thermal activation energy of the process and T is temperature. Characteristic MN energy $E_0 = 1/b$ and isokinetic (critical) temperature $T_0 = E_0/k$ are usually introduced. Thus equations (4) can be rearranged as follows

$$X = X_{00}\exp\Big[\frac{E}{k}\Big(\frac{1}{T_0} - \frac{1}{T}\Big)\Big]\,. \qquad (5)$$

Considering the general equations (2), (4) and (5) we can rewrite the relations for the time constant τ of the relaxation from deep level as follows:

$$\tau = \frac{\tau'_0}{T^2}\exp\Big(\frac{E}{kT}\Big), \quad \tau'_0 = \tau'_{00}\exp\Big(-\frac{E}{E_0}\Big), \quad (6\mathrm{a,b})$$

$$\text{and } \tau = \frac{\tau'_{00}}{T^2}\exp\Big[\frac{E}{k}\Big(\frac{1}{T} - \frac{1}{T_0}\Big)\Big], \qquad (6\mathrm{c})$$

where τ'_{00} is temperature and energy independent constant. It may be evident from Eq. (6c) that the time constant τ does not depend on energy when temperature $T = T_0$. Then a simple relation $\tau'_{00} = T_0^2 t_1/\ln 2$ is valid.

There is a straightforward generalisation of the previous formalism for a charge transient from deep levels continuously distributed in energy [16]. The QDLTS signal for continuous deep levels distribution $G(E)$ in the range of $\langle E_1, E_2\rangle$ is given by the integration of Eq. (1) over the energy:

$$\Delta Q = \Delta Q_0 \int_{E_1}^{E_2}\Big[\exp\Big(-\frac{t_1}{\tau}\Big) - \exp\Big(-\frac{t_2}{\tau}\Big)\Big]G(E)\mathrm{d}E\,, \quad (7)$$

where ΔQ_0 is the amplitude of the charge transient. We note that the factor of the spatial sensitivity is omitted in this simplified formula (7). For QDLTS technique, the factor is proportional to $1 - x/w$, where w is the width of the depletion region in the semiconductor and x is coordinate perpendicular to the top electrode. Therefore, this description is suitable in the case of energy distribution $G(E)$ located in a narrow space sheet, *eg*, interface states at the oxide/semiconductor interface. The following calculations demonstrate how the presence of the MNR affects QDLTS spectra described by formula (7). The calculations are performed with a box-shaped distribution $G(E)$ either without or with the MNR present.

Figure 1 shows a maximum squeezing of the QDLTS spectrum for a box-shaped distribution $G(E)$ if the maximum of the QDLTS spectrum is at the temperature

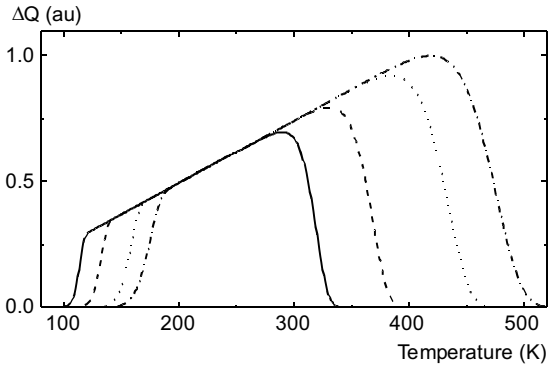

Fig. 3. QDLTS spectra calculated for a box-shaped energy distribution function $G(E)$ in the interval of $\langle 0.3, 0.9\rangle$ eV without consideration of the MNR. Other parameters: $\tau'_{00} = 10^{-10}\,\mathrm{sK}^2$, the sampling time t_1: 10^{-1} s (full line), 10^{-3} s (dashed line), 10^{-5} s (dotted line), 10^{-6} s (dash-dotted line), and $t_2 = 2t_1$.

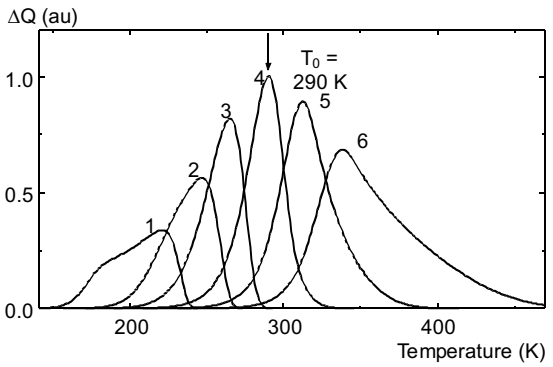

Fig. 4. Fig. 4 Squeezing and distortion of QDLTS spectra due to the MNR present calculated for a box-shaped energy distribution function $G(E)$ in the interval of $\langle 0.3, 0.9\rangle$ eV. Other parameters: $E_0 = 25$ meV, $\tau'_{00} = 1\,\mathrm{sK}^2$,the sampling time t_1: 10^{-1} s (1), 10^{-3} s (2), 10^{-4} s (3), 10^{-6} s (4), 10^{-6} s (5), 10^{-7} s (6), and $t_2 = 2t_1$.

$T_\mathrm{m} = T_0$. Since the difference $(\frac{1}{T} - \frac{1}{T_0})$ in the exponent of Eq. (6c) around the temperature T_m is very small, the time constant τ is weakly energy dependent and the QDLTS spectrum is similar to those obtained for a discrete energy level. Differences between QDLTS spectra of discrete and distributed energy levels are of the order of experimental error. If the QDLTS spectrum lies below T_0, there is a general rule — the lower the energy of individual components of the distribution $G(E)$, the lower the temperature of the contributed component to the total QDLTS spectrum (Fig. 2). This can be considered as a common behaviour of the QDLTS spectra because the factor $(\frac{1}{T} - \frac{1}{T_0})$ in exponent of Eq. (6c) is positive, the same as for the case without consideration of the MNR. When the spectrum lies at temperatures above T_0, the factor $(\frac{1}{T} - \frac{1}{T_0})$ is negative and an opposite effect is found — the lower the energy of the component in $G(E)$, the higher the temperature position in QDLTS spectrum (Fig. 2).

The above mentioned reasoning offers a convenient way how to detect the impact of the MNR on QDLTS spectra. It consists in measurements of the FWHM of the QDLTS spectra for different values of the sampling time t_1. If the MNR is not present, both the FWHM and the height of the QDLTS peak continuously increase with shortening the time t_1 (Fig. 3). If the MNR is present, the dependence of the FWHM *versus* time t_1 shows a more complex behaviour (Fig. 4). The QDLTS spectrum is maximally squeezed at the isokinetic temperature T_0 and the height of the QDLTS peak reaches a maximum value at this temperature (see Fig. 4). Thus, the check of the FWHM of QDLTS spectra using a set of sampling times t_1 may be regarded as a simple test for the presence of the MNR. This analysis relates to the response from a wide energy interval of the gap states, *ie*, in the case of large-pulse excitations. Such a response corresponds to a broad and relatively featureless QDLTS spectrum which does not give possibility to determine the characteristic MN energy E_0. A convenient way how to solve this task is to measure small-signal QDLTS where a continuum of interface states is excited with pulses comparable with kT/q, where q is the electronic charge. Unlike featureless large-signal QDLTS spectra, the emission originates from a limited fraction of the energy gap states. As a result the QDLTS response can be treated as that from a quasi-discrete level, allowing the application of the usual Arrhenius' plot for the determination of the trap parameters [13]. If the quiescent gate voltage U_g changes to a higher reverse bias, the crossover of the surface Fermi level E_F with a component of the interface states moves deeper in the forbidden gap. Thus, a small-signal QDLTS peak measured at different voltages U_gi is made for a probe of the interface states continuum. Having the couples $[E_\mathrm{i}, \tau'_{0\mathrm{i}}]$ determined by the described procedure, we can construct the dependence $\ln \tau'_{0\mathrm{i}}$ *versus* E. If the MNR is present, couples should obey relation (6b) and MN energy E_0 with energy independent prefactor τ_{00} can be yielded from Arrhenius' plot $\ln \tau'_0 - E/E_0$.

3 EXPERIMENTAL

To confront the previous simulations with experimental data, QDLTS measurements were carried out on two MOS samples with a continuum of interface states. It means that these states are confined in a narrow interface region below the oxide and their energy distribution can be probed by the shift of the surface Fermi level, which is related to the change of the gate voltage. The first MOS sample was prepared on a $\langle 100\rangle$ oriented p-type c-Si substrate with a doping concentration of $N_\mathrm{a} = 2\times10^{15}\mathrm{cm}^{-3}$. There was detected no bulk trap on the Schottky barrier with QDLTS technique. An oxide layer with a thickness of 105 nm was grown by thermal oxidation in HCl vapours at 950 °C. As a semiconductor layer of the second MOS sample, an undoped a-Si:H film was deposited by glow discharge on n^+ crystalline Si substrate. The thickness of the a-Si:H layer was 1 μm and the bulk defect density, determined by electron paramagnetic resonance,

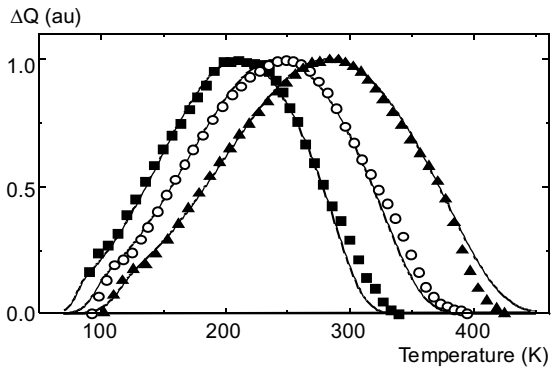

Fig. 5. Experimental QDLTS spectra obtained on p-type c-Si based MOS structure ($t_1 = 7$ ms (squares), $t_1 = 0.7$ ms (open circles), and $t_1 = 0.07$ ms (up triangles)) for large excitation pulses $\Delta U = -0.3$ V and the best fit (full lines) for a Gaussian energy distribution function $G(E)$ without consideration of the MNR calculated with the following parameters: energy interval $\langle 0.09, 0.41\rangle$ eV, maximum $E_{\text{gauss}} = 0.25$ eV and the width $\sigma = 0.10$ eV of the energy distribution, $\tau_0' = 1.17 \times 10^{-4}\,\text{sK}^2$, and $t_2 = 2t_1$.

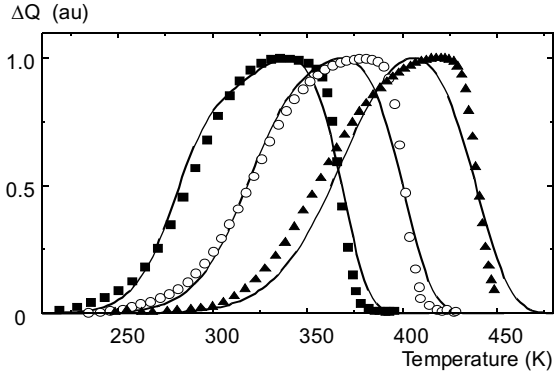

Fig. 6. Experimental QDLTS spectra obtained on a-Si:H based MOS structure ($t_1 = 7$ ms (squares), $t_1 = 0.7$ ms (open circles), and $t_1 = 0.07$ ms (up triangles)) for large excitation pulses $\Delta U = 3$ V and the best fit (full lines) for a box-shaped energy distribution function $G(E)$ considering the MNR with the following parameters: energy interval $\langle 0.39, 0.87\rangle$ eV, $\tau_{00}' = 0.46\,\text{sK}^2$, $E_0 = 43$ meV, and $t_2 = 2t_1$.

was $5 \times 10^{15}\,\text{eV}^{-1}\text{cm}^{-3}$. The oxide/a-Si:H interface was formed by plasmatic anodic oxidation through a thin aluminium overlayer [26]. The oxide thickness was around 50 nm. Before both of the oxidations, there was applied no additional surface treatment. MOS structures were obtained by evaporation of top aluminium contacts of area $3.4 \times 10^{-7}\,\text{m}^2$ on both samples.

In order to probe the interface states in a wide range of energies, the gate voltage U_{g} should be changed in a range as wide as possible. If the formula (7) is to be applied for interpreting the measured QDLTS spectra, the quiescent gate voltage has to be adjusted within the values belonging to the condition of the depletion layer. Voltages from -1.3 V to -1 V and from -1 V to 2 V met this condition for c-Si and a-Si:H based MOS structures, respectively. In the case of the large-pulse excitation we therefore used the bias voltage of -1 V with pulses of -0.3 V for c-Si sample and -1 V with pulses of 3 V for a-Si:H sample. The criteria of the small-pulse excitation for probing the interface states refers to the change of the surface Fermi level E_{F} determined by the change of the gate voltage ΔV_{g}. Considering the interface state density N_{SS} of the order of 10^{11}–$10^{12}\,\text{eV}^{-1}\text{cm}^{-2}$ for applied oxidation procedures, this criterion changes with the density of interface states. Under assumption of a constant $N_{\text{SS}}\,[\text{eV}^{-1}\text{m}^{-2}]$, these changes relate according to [27] as

$$\Delta E_{\text{F}} = \frac{C_{\text{ox}}}{qN_{\text{SS}}}\Delta V_{\text{g}}\,, \tag{8}$$

where C_{ox} is the capacitance per area of the oxide layer. This relation implies that the criterion of small pulses depends on the values of the oxide capacitance and N_{SS}. If the interface states density N_{SS} in the gap increases, the response of the surface potential to the applied bias voltage decreases and a narrower part of the gap is exited. To keep the condition of small-pulse excitation on c-Si and a-Si:H samples, we used the voltage steps of 40 and 100 mV, respectively.

4 RESULTS AND DISCUSSION

We started with QDLTS measurements performed with large-pulse excitation. This is the regime where the presence of the MNR should be argued from the evolution of the FWHM of the QDLTS spectra with changing the sampling time t_1. An example of such large-signal QDLTS spectra on both samples under investigation are shown for three values of t_1 (7, 0.7, 0.07 ms) in Figs. 5 and 6. The FWHM of the QDLTS spectra measured on the MOS structure with c-Si (Fig. 5) become broader with shortening the sampling time t_1. This is a typical behavior, expected from the simulations, for the QDLTS spectra originated from a continuum of gap states with the energy independent exponential prefactor τ_0. By contrast, there is observed no broadening of the QDLTS spectra of the MOS structure on a-Si:H (Fig. 6), which indicates that the MNR is present.

For fitting the previous experimental spectra through the use of the formula (7), we need to know more detailed information on the energy dependence of $\tau_0' = f(E)$, the energy limits E_1, E_2 of the interface states continuum contributed to the signal, and the shape of its distribution $f(E)$. This information was obtained by the small-signal QDLTS technique and these parameters were used as an initial guess for fitting. In this case, traps from a narrow energy interval around the Fermi level can only respond and higher resolutions in both energy and space are reached [28]. It should be noted that the interface states are investigated in the energy range imposed by the applied voltage range. Sets of relevant QDLTS spectra taken at different bias voltages are depicted in Figs. 7 and 8 for c-Si and a-Si:H based MOS structures, respectively. In spite of using the small-pulses, the records for the thermal oxide/c-Si interface do not remind QDLTS peaks of quasi-discrete energy levels because their FWHMs are broader than the ideal line shape for monoenergetic response. The

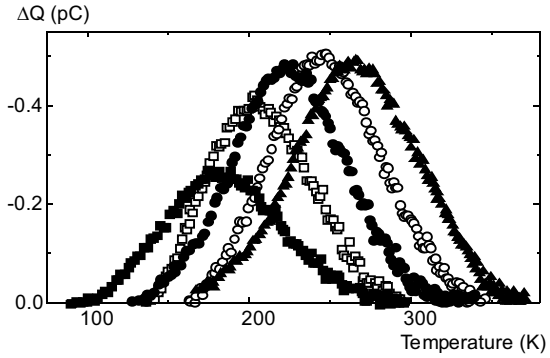

Fig. 7. Experimental QDLTS spectra of c-Si based MOS structure for small excitation pulses $\Delta U = -0.04$ V and different bias voltages U: -1.3 V (squares), -1.2 V (open squares), -1.1 V (circles), -1.05 V (open circles), and -1.0 V (triangles), $t_1 = 7$ ms and $t_2 = 2t_1$.

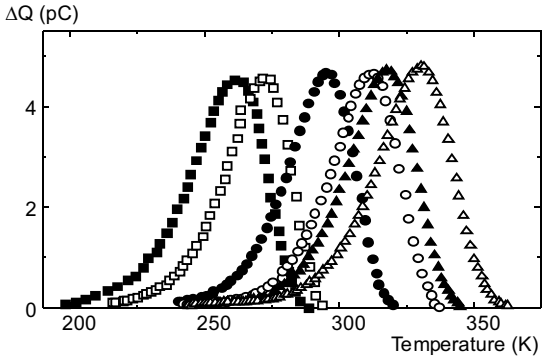

Fig. 8. Experimental QDLTS spectra of a-Si:H based MOS structure for small excitation pulses $\Delta U = 0.1$ V and different bias voltages U: 1.9 V (squares), 1.4 V (open squares), 0.7 V (circles), 0 V (open circles), -0.5 V (triangles), and -0.9 V (open triangles), $t_1 = 7$ ms and $t_2 = 2t_1$.

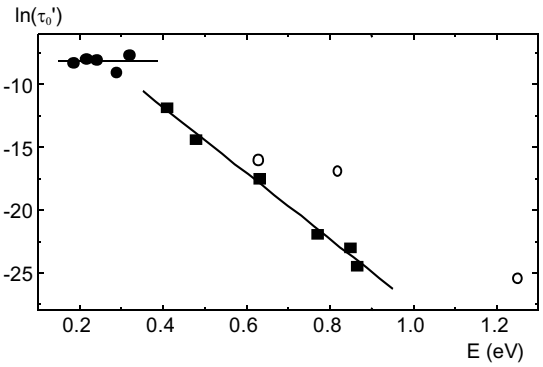

Fig. 9. Arrhenius' plots for determination of an energy dependence of the exponential prefactor τ_0'. Full circles and squares correspond to data obtained by small-signal QDLTS measurements on c-Si and a-Si:H based MOS structures, respectively. As a result of the linear regression (full lines), the following parameters were obtained: the energy independent $\tau_0' = 3 \times 10^{-4}\,\mathrm{sK}^2$ for c-Si sample and the MN energy $E_0 = 38$ meV with $\tau_{00}' = 0.25\,\mathrm{sK}^2$ for a-Si:H sample. Open circles show data reported by Nádaždy *et al* [11].

measured QDLTS peaks can be fitted with a band of energy levels about 50 meV broad. The broadening of the QDLTS peaks is caused by surface fluctuations induced by a charge inhomogeneity at the oxide/c-Si interface [29] and/or extension of defect states under this interface toward the bulk of the semiconductor. Nevertheless, it is possible to read the maxima of peaks for different rate windows and construct the Arrhenius' plot. The a-Si:H sample is characterized by distinct QDLTS peaks (Fig. 8), which can be fitted by discrete energy levels. The shift of QDLTS peaks in Figs. 7 and 8 to higher temperatures for larger reverse voltages corresponds to a change of the position in the energy scale defined by the intersection between the surface Fermi level E_F and the interface states. The activation energy and exponential prefactor τ_0' for individual peaks were determined by the standard Lang's approach, *ie*, by the Arrhenius' plot $\ln \tau_\mathrm{m} T_\mathrm{m}^2$ *versus* $1/T_\mathrm{m}$, where τ_m corresponds to the inverse of the rate window. There were used six rate windows between 100 and $10000\,\mathrm{s}^{-1}$. Sets of couples $[E, \tau_0']$ obtained for both samples are summarized in Tab. 1 and dependences of $\ln \tau_0'$ *versus* E are plotted in Fig. 9. The continuum of gap states at thermal oxide/c-Si interface is characterized by an energy independent $\tau_0' = 3 \times 10^{-4}\,\mathrm{sK}^2$. If the interface states of a-Si:H sample are affected by the MNR present, these couples should obey Eq. (6) and the MN energy E_0 could be determined from the slope of the Arrhenius' plot $\ln \tau_0' = \ln \tau_{00}' - E/E_0$. In fact, experimental data (full squares in Fig. 9) fall in with a straight line, which yields the MN energy $E_0 = 0.38$ eV and $\tau_{00}' = 0.25\,\mathrm{sK}^2$. The shape of the distribution of c-Si based MOS structure for fitting was reconstructed from the QDLTS peak maxima ΔQ_max according to [26] as

$$\Delta Q_\mathrm{max} = \frac{1}{4} \frac{C_\mathrm{ox}}{C_\mathrm{ox} + C_\mathrm{S}} A q N_\mathrm{SS} \Delta E_\mathrm{F}\,, \tag{9}$$

where C_S is the capacitance of the depletion region of the semiconductor and A is the area of the top electrode. The factor $1/4$ originates from the carry of the boxcar filter $\exp(-t_1/\tau) - \exp(-t_2/\tau)$. A narrow energy increment ΔE_F is assessed via the following approximation

$$\Delta E_\mathrm{F} = q \Delta \Phi_\mathrm{S} \approx q\Big(1 - \frac{C_\mathrm{lf}}{C_\mathrm{ox}}\Big) \Delta V_\mathrm{g}\,, \tag{10}$$

where C_lf is the low frequency capacitance and $\Delta\Phi_\mathrm{S}$ denotes the related change of the surface potential of the semiconductor. In this way we arrived at the N_SS distribution which can be approximated over the range of investigated energies by a Gaussian function $N_\mathrm{SS}^0 \exp\big(-(E-0.24)^2/0.02\big)$. There is a serious difficulty concerning the practical utilization of the formula (9) for undoped a-Si:H due to the inherent energy and spatial distribution of the bulk density of gap states, which makes obscure the definition of both capacitances C_S and C_lf needed to assess the quantity of the factor $C_\mathrm{ox}/(C_\mathrm{ox}+C_\mathrm{S})$ and ΔE_F, respectively. According to the improved defect-pool models [30 and 31], the gap states distribution for undoped a-Si:H in the range of observed energies does not change essentially. Therefore, a box-shaped energy distribution function $N_\mathrm{SS}(E)$ was taken for fitting the

Table 1. Values of E and τ_0' for quasi-discrete energy components of interface states obtained by the small-signal QDLTS method on c-Si and a-Si:H based MOS structures, respectively. U_g stands for bias voltage used to shift the surface Fermi level and chooses particular component of the interface states.

Thermal oxide/c-Si						
U_g (V)	-1.3	-1.2	-1.15	-1.1	-1	
E (eV)	0.18	0.21	0.24	0.29	0.32	
τ_0' (sK^2)	2.66×10^{-4}	3.61×10^{-4}	3.33×10^{-4}	1.27×10^{-4}	4.95×10^{-4}	
Plasmatic oxide/a-Si:H						
U_g (V)	1.9	1.4	0.7	0	-0.5	-0.9
E (eV)	0.41	0.48	0.63	0.77	0.85	0.87
τ_0' (sK^2)	7.43×10^{-6}	5.66×10^{-7}	2.60×10^{-8}	3.09×10^{-10}	1.02×10^{-10}	2.48×10^{-11}

experimental data of a-Si:H sample. Large-signal QDLTS spectra of both samples were fitted with the following parameters: energy interval $\langle E_1, E_2\rangle$ of $N_{SS}(E)$ contributed to the response, exponential prefactors τ_0' or τ_{00}' with E_0. As an initial guess for fitting the spectra, the values of parameters obtained by the small-signal QDLTS technique were used. The QDLTS spectra shown in Figs. 5 and 6 with solid lines were calculated for the best fit with the following values: $\langle 0.08, 0.42\rangle$ eV, $\tau_0' = 3.3 \times 10^{-4}$sK^2 for c-Si sample and $\langle 0.41, 0.87\rangle$ eV, $\tau_{00}' = 0.46\,\mathrm{sK}^2$, and $E_0 = 43$ meV.

There are some discrepancies related to the values of the parameters obtained by fitting the large-signal QDLTS spectra and those determined by the small-signal QDLTS technique. The former QDLTS spectra could be influenced by other effects which are not taken into account in our calculations. For example, the approximate formula (7) is no longer valid in the case of high-density N_{SS} and a deviation from this approximation can be expected for N_{SS} of the order of 10^{11}–10^{12}eV^{-1}cm^{-2} [27]. Since the small-signal QDLTS spectra are taken close to an equilibrium state, we consider this method more reliable for determination of the defect states parameters. Critical temperature for the MN energy $E_0 = 38$ meV is $T_0 = 441$ K. This relatively high temperature is the reason why we are not able to see the maximal squeezing of the QDLTS spectra in the temperature range used at our measurements.

It is worth mentioning that the large-signal DLTS spectrum is proportional to the shape of $G(E)$ and after proper scaling the spectrum can be used as a first trail function for fitting this spectrum [9]. Since the MNR present induces a change of the exponential prefactor τ_0' by several orders, this should be taken into account for a correct temperature — energy transformation of the QDLTS spectrum. Knowing the value of MN energy E_0, we can correctly transform the temperature to the energy scale by the inverse of relation (6c)

$$E = \frac{E_0}{E_0 - kT} kT \ln\Big(\frac{T^2 \tau_m}{\tau_{00}'}\Big), \qquad (11)$$

where τ_m is the QDLTS rate window. It means that the smaller difference $E_0 - kT$, the higher compression of the energy scale.

Experimental evidences of the MNR effect on the emission process in a-Si:H were already reported in some papers [11, 19, and 32]. The MNR present was noted for QDLTS spectra of undoped a-Si:H [11]. The authors observed three QDLTS peaks, in dependence on bias annealing at equilibration temperature of 490 K applied to the sample before measurement. The activation energies of these peaks were 0.63, 0.82, and 1.25 eV, which correspond to the mean energies of the components of the gap states predicted by the improved defect-pool models [30, 31]. Three open squares in Fig. 9 depict these energies *versus* exponential prefactor τ_0'. They do not fit full the line obtained as a linear regression of our data of a-Si:H based MOS structure. Unlike Ar bombardment procedure [11, 33], the insulating layer of our samples was prepared by plasmatic anodic oxidation through a thin aluminum overlayer [26]. The former procedure [11, 33] leads to a decrease of the density of the gap states at the subsurface region of a-Si:H, which allowed detection of the gap states from the bulk. Small-signal QDLTS spectra of our sample indicate that the measured signal arises from a narrow spatial region of a-Si:H layer adjacent to the interface with a plasmatic oxide. Therefore, we attribute the difference between the previous and present dependences of τ_0' on energy to different spatial localization of the measured signal and/or modification of the electrical properties of a-Si:H at the interface by plasmatic anodic oxidation.

Kondo with co-workers [19] investigated the effect of the MNR on the electrical conductivity of a-Si:H measured on thin film transistors. The layer of a-Si:H was prepared on a thermally oxidized n^+ c-Si substrate by plasma enhanced chemical vapour deposition followed by evaporation of Mg electrodes. They observed the energy dependence of the sheet conductance with the MN energy of 40 meV which coincides with the value of 38 meV presented in this paper. On the other hand, Yan and Andriaenssens [35] found by post-transit photocurrent analysis on p-i-n structures the MN energy of 30 meV. This value was determined in a narrow energy range from 0.42 to 0.52 eV from four points corresponding to different samples, which implies a higher experimental error.

5 CONCLUSIONS

It has been demonstrated how the MNR, considered via the energy dependence of the exponential prefactor τ_0' of the charge emission rate from the gap states continuously distributed in energy, influences QDLTS spectra. Computer simulations showed that the main feature of large-signal QDLTS spectra influenced by the MNR is the absence of the broadening of the spectra with increasing the rate window. This behavior was observed for the gap states at the plasma oxide/a-Si:H interface. On the other hand, QDLTS spectra of the thermal oxide/c-Si interface became broader with increasing the rate window, which is characteristic for energy independent prefactor τ_0'. This kind of measurement is suggested as an indicator of the MNR present. To obtain values of the MN energy E_0 and energy independent prefactor τ_{00}', the small-signal QDLTS method is to be used. In this case, interface states are probed in a narrow energy interval and the corresponding QDLTS peaks can be treated as quasi-discrete ones. In addition, an advantage over the large-pulse excitation is that the sample under test remains close to the thermodynamic balance throughout the measurement. Using different bias voltages U_{gi}, a set of couples $[E_{\mathrm{i}}, \tau_{0\mathrm{i}}']$ was obtained and E_0 with τ_{00}' were yielded from Arrhenius' plot $\ln \tau_0' - E/E_0$. Knowing these parameters is crucial for a correct transformation of the temperature scale of the QDLTS spectrum to the energy scale of the gap states distribution $G(E)$.

Acknowledgement

This work was partly supported by the VEGA grant agency of the Slovak Republic under project No. 2/1013 /21.

References

[1] LANG, D. V.: J. Appl. Phys. **45** (1974), 3023.

[2] LEFÉVRE, H.—SCHULTZ, M.: Appl. Phys. **12** (1977), 45.

[3] CHANTRE, P.—VINCENT, G.—BOIS, D.: Phys. Rev. B. **23** (1981), 5335.

[4] KIROV, K. L.—RADEV, K. B.: Phys. Stat. Sol. (a) **63** (1981), 711.

[5] FARMER, J. W.—LAMP, C. D.—MEESE, J. M.: Appl. Phys. Lett. **44** (1982), 1063.

[6] FOURCHES, N.: Appl. Phys. Lett. **58** (1991), 364.

[7] YAMASAKI, K.—YOSHIDA, M.—SUGANO, T.: Jpn. J. Appl. Phys. **18** (1979), 113.

[8] CHANTRE, P.: Appl. Phys. A **48** (1989), 3.

[9] LANG, D. V.—COHEN, J. D.—HARBISON, J. P.: Phys. Rev. B **25** (1982), 5285.

[10] CRANDALL, R. S.: Phys. Rev. B **36** (1987), 2645.

[11] NÁDAŽDY, V.—DURNÝ, R.—PINČÍK, E.: Phys. Rev. Lett. **78** (1997), 1102.

[12] HROBÁR, M.—GRENDEL, M.—THURZO, I.: Phys. Stat. Sol. (a) **82** (1984), 519.

[13] LANG, D. V.: Thermally Stimulated Relaxation in Solids, Vol. 37 of Topics in Applied Physics, edited by P. Brauhlich, Springer, Berlin (1979).

[14] MEYER, A.—NELDEL, H.: Z. Tech. Phys. **12** (1937), 588.

[15] THURZO, I.—GMUCOVÁ, K.: Phys. Stat. Sol. (a) **160** (1997), 89.

[16] KLUVÁNEK, P.—BARANČOK, D.—KELEŠI, L.: J. Electrical Engineering **51** (2000), 51.

[17] JACKSON, W. B.: Phys. Rev. B **38** (1988), 3595.

[18] OVERHOF, H.—THOMAS, P.: Electronic Transport in Hydrogenated Amorphous Semiconductors, Springer-Verlag, New York, 1989.

[19] KONDO, M.—CHIDA, Y.—MATSUDA, A.: J. Non-Cryst. Solids **198-200** (1996), 178.

[20] NARASIMHAN, K.—ARORA, B. M.: Solid State Commun. **55** (1985), 615.

[21] ALMOND, D. P.—WEST, A. R.: Solid State Ionics **23** (1987), 27.

[22] CRINE, J.-P.: IEEE Trans. Electr. Insul. **26** (1991), 811.

[23] EXNER, O.: Coll. Czech. Chem. Commun. **37** (1972), 1425.

[24] YELON, A.—MOVAGHAR, B.: Phys. Rev. Lett. **65** (1990), 618.

[25] YELON, A.—MOVAGHAR, B.—BRANZ, H. M.: Phys. Rev. B **46** (1992), 12244.

[26] BARTOŠ, J.—PINČÍK, E.: Thin Solid Films **247** (1994), 178.

[27] MURRAY, F.—CARIN, R.—BOGDANSKI, P.: J. Appl. Phys. **60** (1986), 3592.

[28] NÁDAŽDY, V.—THURZO, I.: Phys. Stat. Sol. (a) **127** (1991), 167.

[29] TREDWELL, T. J.—VISWANATHAN, C. R.: Solid-State Electron. **23** (1980), 1171.

[30] POWELL, M. J.—DEANE, S. C.: Phys. Rev. B **48** (1993), 10815.

[31] SCHUMM, G.: Phys. Rev. B **49** (1994), 2427.

[32] YAN, B.—ANDRIAENSSENS, G. J.: J. Appl. Phys. **77** (1995), 5661.

[33] DURNÝ, R.—PINČÍK, E.—NÁDAŽDY,V.—JERGEL, M.—SHIMIZU, J.—KUMEDA, M.—SHIMIZU, T.: Appl. Phys. Lett. **77** (2000), 1783.

Received 15 August 2001

Peter Kluvánek (Mgr), born in Trenčín, Slovakia, in 1974, graduated from the Faculty of Mathematics and Physics, Comenius University. Since 1997 he has been a doctorate student at the Department of Physics, Faculty of Electrical Engineering and Information Technology, Slovak Univesity of Technology, the topic of his work is "Defects in amporphous hydrogenated silicon - theoretical and experimental methods".

Drahoslav Barančok (Doc, Ing, CSc), born in Jasenie, near Banská Bystrica, in 1945, graduated from the Faculty of Electrical Engineering, Slovak University of Technology, Bratislava, in solid state physics, in 1968 and received the CSc (PhD) degree in experimental physics in 1977. At present he is Associate Professor for physics, Department of Physics, Faculty of Electrical Engineering and Infomation Technology, Slovak University of Technology, Bratislava. Research experience and interest: optical thin films, electrical transport in noncrystalline solids, ultra-thin macromolecular films and molecular electronics.

Vojtech Nádaždy (Ing, CSc) was born in Bratislava, Slovakia, in 1961. He graduated in microelectronics from the Faculty of Electrical Engineeering, Slovak University of Technology, and since 1986 he has been with the Insitute of Physics of Slovak Academy of Sciences. The topics of his professional interest are semiconductor physics, theory, experimental methods applications.